# Altering the pathway of immunoglobulin hypermutation by inhibiting uracil-DNA glycosylase

**Javier Di Noia & Michael S. Neuberger**

*Medical Research Council Laboratory of Molecular Biology, Hills Road, Cambridge CB2 2QH, UK*

**A functional immune system depends on the production of a wide range of immunoglobulin molecules. Immunoglobulin variable region (IgV) genes are diversified after gene rearrangement by hypermutation. In the DNA deamination model, we have proposed that deamination of dC residues to dU by activation-induced deaminase (AID) triggers this diversification. In hypermutating chicken DT40 B cells, most IgV mutations are dC → dG/dA or dG → dC/dT transversions, which are proposed to result from replication over sites of base loss produced by the excision activity of uracil-DNA glycosylase. Blocking the activity of uracil-DNA glycosylase should instead lead to replication over the dU lesion, resulting in dC → dT (and dG → dA) transitions. Here we show that expression in DT40 cells of a bacteriophage-encoded protein that inhibits uracil-DNA glycosylase shifts the pattern of IgV gene mutations from transversion dominance to transition dominance. This is good evidence that antibody diversification involves dC → dU deamination within the immunoglobulin locus itself.**

The DNA deamination model[1] suggests that the initial event in IgV gene diversification is deamination of dC residues within the IgV gene by AID[2]. The pathway employed for resolving the resultant dU/dG mismatch will then determine the precise nature of the diversification. Thus, replication templated on the dU/dG mismatch will lead to transitions at dC/dG (phase 1A mutation) (Fig. 1a). However, uracil residues in DNA are substrates for base excision repair[3], and the action of a uracil-DNA glycosylase[4] on the uracil will generate an abasic site (a site of base loss). Replication past this abasic site will result in dC → dA/dG/dT and dG → dA/dC/dT mutations. The precise pattern of nucleotide substitutions in this situation will probably depend on the preferences of the DNA polymerase involved but, given that two of the three possible substitutions are transversions, a transversion predominance is likely to ensue (phase 1B hypermutation). We have further envisaged that binding to the dU/dG mismatch (or to some intermediate in its repair) by the MSH2/MSH6 recognition complex could lead to error-prone patch repair, yielding mutations at dA/dT (phase 2 hypermutation), whereas recombination-mediated repair templated on an IgV pseudogene could lead to IgV gene conversion[1].

A critical test of this model would be provided by determining whether the hypermutation pathway could be perverted by inhibition of uracil-DNA glycosylase activity. In the case of phase 2 hypermutation and gene conversion, it is difficult to anticipate the effects of inhibiting uracil-DNA glycosylase because we do not know whether these pathways are triggered by the dU/dG mismatch itself or are triggered only after the generation of an abasic site. However, with regard to phase 1 hypermutation, it is clear that phase 1B mutation (templated on the abasic site) should be blocked by inhibition of uracil-DNA glycosylase activity, whereas phase 1A mutation (templated on the dU/dG itself) should be unaffected. Chicken DT40 B cells that lack the DNA-repair gene *XRCC2* (ref. 5) provide an attractive system in which to test this hypothesis because these cells constitutively perform transversion-favoured dC/dG (that is, largely phase 1B) hypermutation at high frequency, with little contribution of phase 2 mutation or gene conversion to IgV gene diversification[6]. More than 90% of the mutations in *XRCC2*-deficient DT40 cells are nucleotide substitutions at dC/dG, with some two-thirds of these substitutions being transversions[6]. The different transversions are not equally favoured but rather suggest that the polymerase involved preferentially inserts dC opposite an abasic site.

## Uracil-DNA glycosylase activity in DT40 cells

We were concerned that it might be difficult to obtain cells deficient in uracil-DNA glycosylase activity. Cytosine deamination is a major form of endogenous DNA damage[7]: inhibiting its repair by blocking all uracil-DNA glycosylase activity might be incompatible with clonal expansion. Gene redundancy might in any case make it difficult to generate glycosylase-deficient cells because there are several genes in the mammalian genome that encode enzymes able to excise uracil from DNA[8]. Indeed, mice carrying disruptions of the major uracil-DNA glycosylase gene (*UNG*, which is homologous to *E. coli ung*) exhibit a relatively mild phenotype[9] and have revealed a backup uracil-excising activity that is probably encoded by the *SMUG1* DNA glycosylase gene[10,11].

We were struck, however, by the fact that we could not detect a *SMUG1* homologue in the well-represented chicken expressed sequence tag (EST) database (http://chick.umist.ac.uk), although ESTs homologous to human *UNG* were readily identified. We analysed the coding sequence of chicken *UNG*—obtained by polymerase chain reaction with reverse transcription (RT–PCR) from DT40 cells (see Supplementary Information)—and found high homology between the chicken and human enzymes. This suggested that it might be possible to inhibit the chicken *UNG* gene product using the uracil-DNA glycosylase inhibitor (Ugi) protein[12,13] encoded by the uracil-containing genome of bacteriophage PSB-2. Ugi inhibits the *ung*-encoded uracil-DNA glycosylase from bacteria as well as from a wide variety of eukaryotic species including humans[12–14]. The sequence of chicken *UNG* (see Supplementary Information) indicated that it retained the critical residues for catalytic activity and Ugi binding[15,16]. This provided a way of ascertaining whether DT40 cells, like mouse cells[11], contain a major back-up activity for the excision of uracil from DNA when the *UNG* gene product is inhibited. No such back-up was apparent. Addition of Ugi to a DT40 cell extract before performing a uracil excision assay on an oligonucleotide substrate resulted in the inhibition of nearly all activity (Fig. 1b). Although this certainly

does not exclude the existence of a back-up uracil-excising activity in DT40 cells (such activity might simply not reveal itself under the particular *in vitro* assay conditions used), the result encouraged us to determine whether IgV gene diversification was affected in DT40 cells carrying a transfected Ugi expression cassette.

### Inhibition of UNG in *Ugi* transfectants of DT40 cells

Electroporation of DT40 cells with a plasmid in which Ugi expression was linked to that of the selective marker by use of an internal ribosome entry site yielded very few transfectants (compared with controls), and those that survived the selection contained no detectable *Ugi* messenger RNA as judged by northern blot analysis (Fig. 1c). Success was, however, achieved with a distinct vector (pEF-Ugi) in which Ugi expression was driven by the elongation factor 1α (EF1α) promoter and the selective marker (hygromycin resistance) was under control of the herpes simplex virus (HSV) thymidine kinase promoter (Fig. 1c). Of 30 clones analysed, all contained detectable *Ugi* mRNA (although at varying levels of abundance) as judged by northern blot. Extracts were prepared from 24 independent pEF-Ugi transfectants (12 from each of two electroporation experiments). All 24 extracts revealed a substantial (>99%) inhibition of uracil-DNA glycosylase

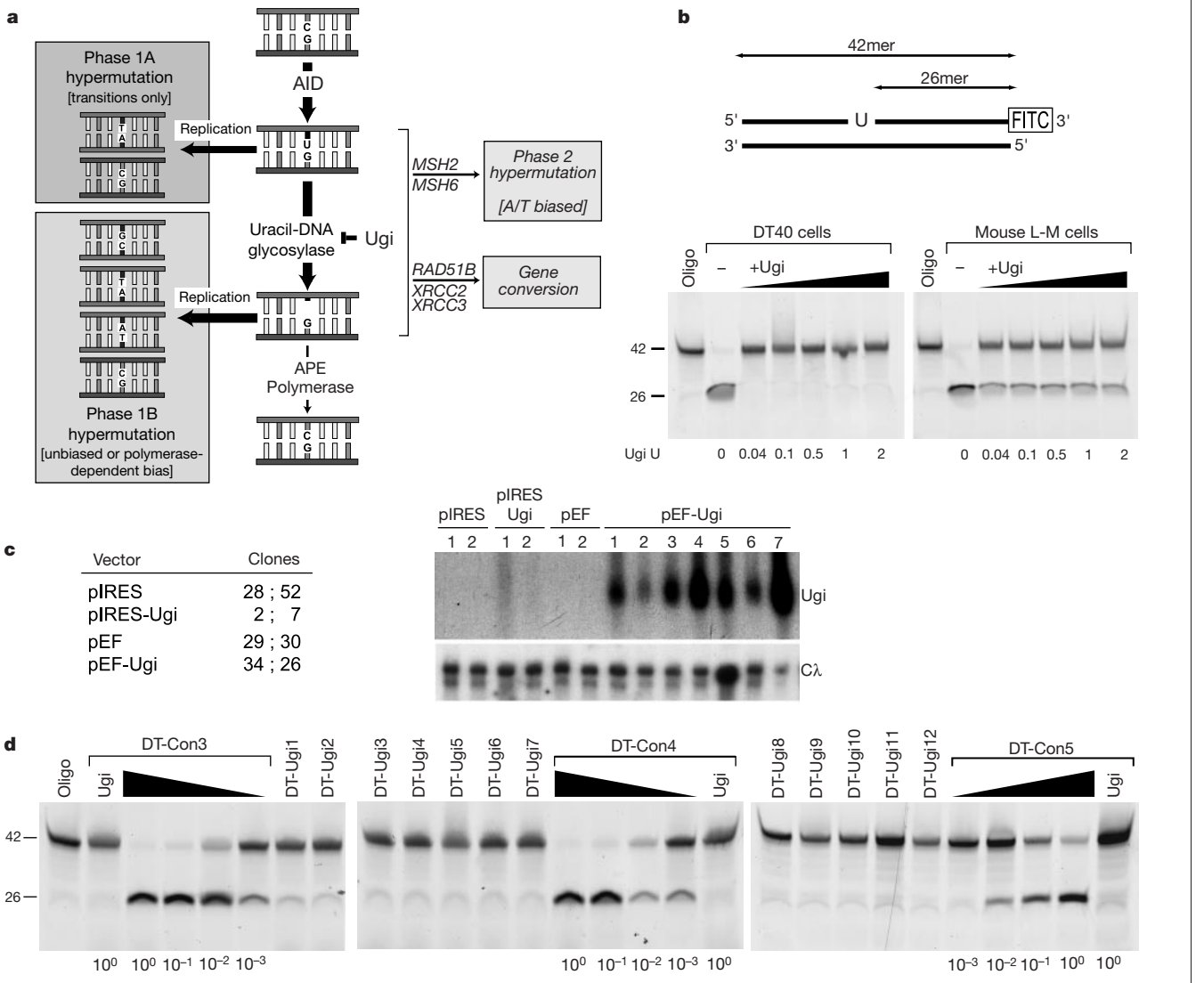


**Figure 1** Uracil-DNA glycosylase activity in the DT40 B-cell line. **a**, The proposed role of uracil-DNA glycosylase in IgV gene diversification in *XRCC2*-deficient DT40 B cells. The major pathway of IgV gene diversification in *XRCC2*-deficient DT40 cells seems to be phase 1B hypermutation; phase 2 hypermutation and IgV gene conversion are minor contributors in these cells (see text) and are therefore indicated in italics. The extent to which the glycosylase-generated abasic site is repaired by an apyrimidic endonuclease (APE) and DNA polymerase (rather than simply acting as a template for replication—phase 1B mutation) is unknown, although work described here suggests that it is not the major pathway. **b**, Ugi inhibition reveals residual uracil-DNA excision activity in extracts of mouse L cells but not in DT40 cells. A fluorescein-labelled oligonucleotide containing a single dU residue was incubated with chicken DT40 or mouse L-M cell extracts (10 μg protein) in the presence of varying concentrations of Ugi (0, 0.04, 0.1, 0.5, 1 and 2 units). The reaction products were resolved on 15% TBE-urea polyacrylamide gels. **c**, Transfection of Ugi expression (and control) vectors into DT40 cells. The number of clones growing in selective medium obtained in two independent transfections performed with pIRES-Ugi and pEF-Ugi (as well as vector-only controls) is shown on the left. *Ugi* mRNA expression in randomly selected transfectants was analysed by northern blot, controlling with an immunoglobulin Cλ probe. No *Ugi* mRNA was detected in any of the pIRES-Ugi transfectants analysed, whereas *Ugi* mRNA was detected (at varying levels) in all pEF-Ugi clones studied. **d**, Uracil-DNA excision activity in pEF-Ugi (and control) transfectants of *XRCC2*-deficient DT40 cells. Activity was monitored in serial dilutions of extracts from control transfectants (DT-Con3, 4 and 5; with 'Ugi' indicating that 2 units of purified Ugi protein were added to the extract at the time the assay was performed) or in undiluted extracts from pEF-Ugi transfectants (DT-Ugi1–12). Assays were performed as in **b** using undiluted extracts (10 μg protein) as well as with tenfold serial dilutions (1:10, 1:100 and 1:1,000) in the case of DT-Con3, 4 and 5.

activity; no such inhibition was evident in 12 control transfectants (Fig. 1d).

### Shifted IgV mutation pattern in *Ugi* transfectants

Somatic hypermutation in DT40 cells can lead to IgV gene inactivation, with such cells being readily identifiable by their loss of surface immunoglobulin M (IgM). Comparison of *Ugi*-transfected *XRCC2*-deficient DT40 clones (DT-Ugi clones) and vector-only control transfectants (DT-Con clones) revealed no difference in the frequency of accumulation of surface IgM (sIgM)-loss variants: analysis of independent clones revealed a median of 5.1% sIgM-loss variants after 25 days in both cases. However, a substantial

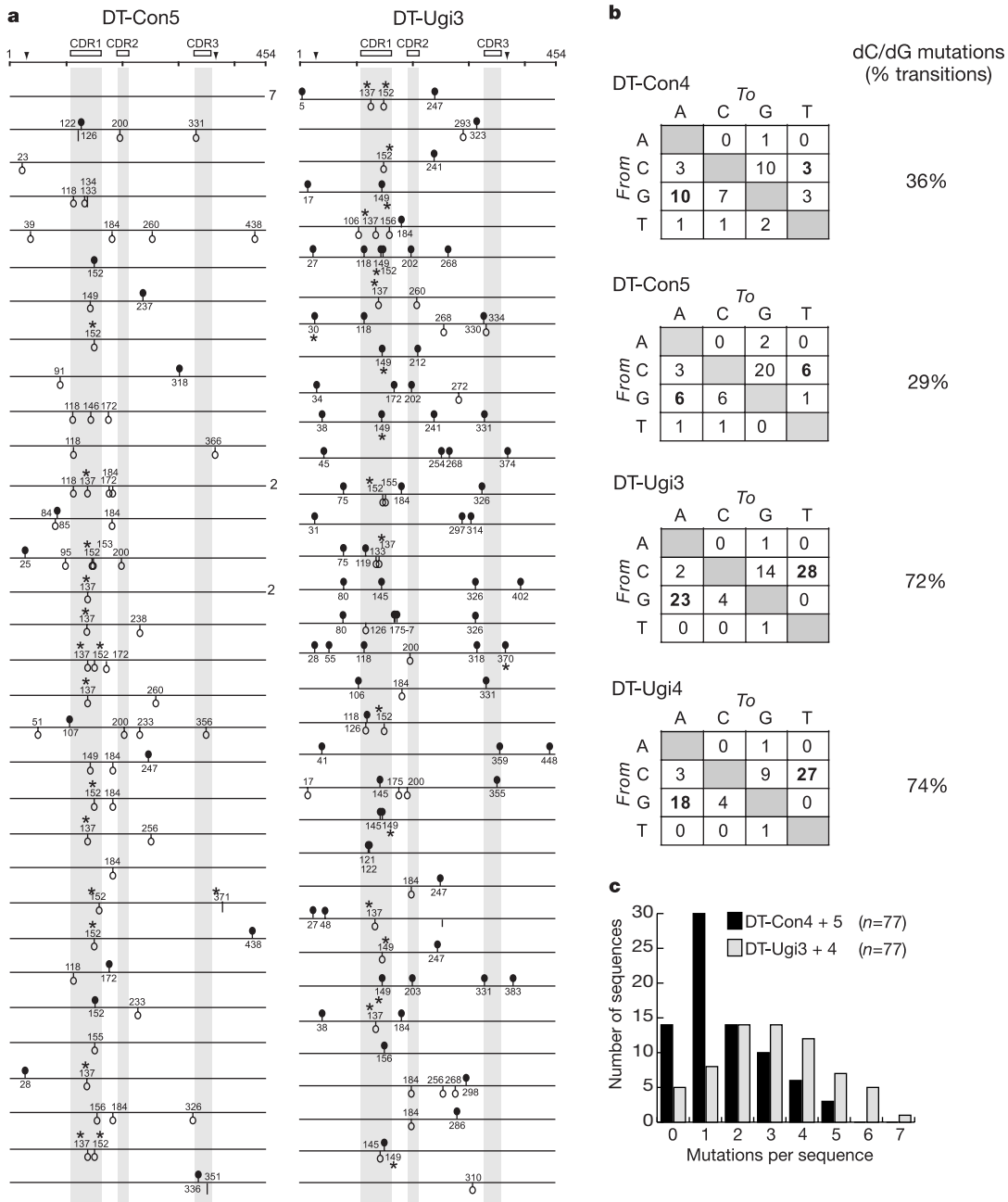


**Figure 2** Analysis of Vλ mutations in surface IgM-loss variants sorted from pEF-Ugi and control transfectants. **a**, Comparison of Vλ sequences in sIgM-loss variants sorted from Ugi-expressing transfectant DT-Ugi3 and control transfectant DT-Con5 after 1 month of clonal expansion. Each horizontal bar represents the rearranged Vλ1/Jλ (numbering as in Fig. 3a). Transitions at dC/dG are indicated by a filled circle above the line, transversions at dC/dG by open circles below the line, and dA/dT mutations by a vertical line. Stop codons and splice site inactivations are indicated by an asterisk. A few Vλ clones of identical sequence were found among the population amplified from the sorted DT-Con5 (but not DT-Ugi3) loss variants; the number of such repeat sequences is indicated by a digit at the right end of the horizontal bar. No gene-conversion events (screened for by the criteria previously applied[6]) were identified in DT-Ugi3 or DT-Con5, although two conversion events and a single base-pair deletion were identified among DT-Ugi4 sequences. **b**, Pattern of nucleotide substitutions. The digits within the tables indicate the number of the relevant substitution events observed. The same mutation when present in different Vλ sequences obtained from a single DT40 transfectant was scored only once. Thus, for example, the dC → dT transition at position 118 in the DT-Ugi3 clone was scored only once although it was observed in three distinct Vλ sequences. This stringent approach to avoiding overcalling mutations in clones that might be dynastically related will result in an undercalling of mutations, especially at mutational hotspots. **c**, Comparison of the mutational load in Vλ sequences obtained from Ugi-expressing (DT-Ugi) and control (DT-Con) clones.

difference was apparent between the two sets of cells when the Vλ sequences among the sorted sIgM-loss variants were compared (Fig. 2). Whereas nucleotide transitions accounted for only a minority of the substitutions at dC/dG in the control transfectants (13 of 36 and 12 of 42 in the two clones analysed), this increased to a majority (51 of 71 and 45 of 61) in the Ugi-expressing transfectants.

The mutation load was also somewhat greater in the two Ugi-expressing transfectants than in the controls (Fig. 2c), averaging 2.9 mutations per Vλ sequence for the sorted sIgM-loss variants from the Ugi-expressing clones, compared with 1.8 mutations per sequence in those obtained from sorted control cells. We suspect that this increased mutation load does not translate into a similar increase in the frequency of sIgM-loss variants because the transition-skewed nature of the base substitutions means that a smaller proportion of mutations lead to IgV gene inactivation. Thus, within the Vλ sequence, there are 17 dC or dG residues that can give rise to a stop codon by a single nucleotide substitution but only 7 of these dC/dGs will yield a stop codon by a transition mutation. This cannot readily be extrapolated into calculating the effects of increased transition bias on the frequency of generation of sIgM-loss variants because not all dC/dGs are targeted equally and mutations other than stop codons in Vλ can lead to loss of sIgM expression. Nevertheless, the comparison is likely to reveal a general tendency.

To ensure that effects of Ugi expression on the mutation pattern were not obscured or skewed by selecting for sIgM-loss variants, we obtained IgVλ sequences from DT-Ugi3, DT-Ugi4, DT-Con4 and DT-Con5 as well as five other Ugi-expressing and five other control transfectants after 3–8 weeks of clonal expansion without imposing any selection for phenotypic changes. The mutations in all seven Ugi-expressing transfectants showed a marked skewing towards nucleotide transitions (Fig. 3 and Table 1). Although only 38% of

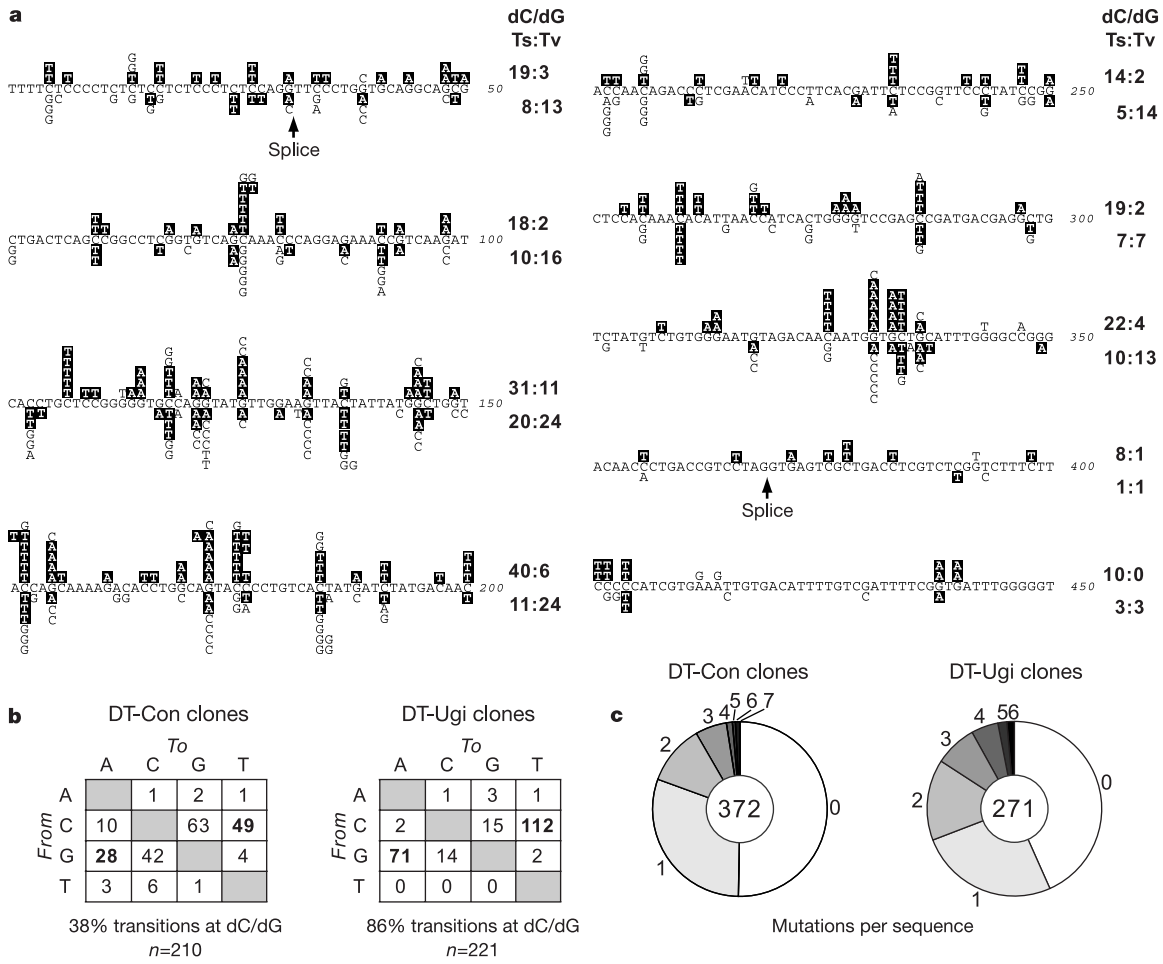


**Figure 3** Analysis of Vλ mutations in unsorted populations of pEF-Ugi and control transfectants after 3–8 weeks of clonal expansion. **a**, Distribution of mutations across Vλ. The consensus Vλ1/Jλ sequence is the best fit to the Vλ sequences obtained from the 14 DT-Ugi and DT-Con clones. Mutations detected in the DT-Ugi-expressing clones are shown above the line, those in the control transfectants below the line, and transitions at dC/dG are shaded black. Adjacent to each line of Vλ sequence, the number of dC/dG transition (Ts) and transversion (Tv) mutations detected in that section of sequence in DT-Ugi (above the line) and DT-Con (below the line) transfectants is indicated. The same stringent criterion described in the legend to Fig. 2b was used to avoid repeat calling of the same mutational event. Only primary mutations are illustrated for reasons of clarity; 13 secondary mutations (6 in the DT-Ugi clones, 7 in the controls) are omitted from this panel and are designated secondary in that the parental clone in which the mutation arose already carried a mutation distinct from the consensus presented here at the relevant position, or where dynastic relationships revealed that a mutated base had remutated during clonal expansion. These secondary mutations are, however, retained in the database underpinning the rest of the analyses. **b**, Pattern of nucleotide substitutions in the Ugi-expressing and control transfectants. The absolute numbers of mutations obtained from the individual Ugi-expressing and control clones (Table 1) have been separately compiled. The same stringent criterion applied in Fig. 2b has been used to avoid counting the same mutational event twice. **c**, Mutation load among the Vλ sequences from Ugi-expressing and control transfectants. The number in the centre of the pie chart is the number of Vλ sequences determined, with each slice of the pie indicating the proportion of sequences with 0–7 mutations. Each distinct Vλ sequence has been scored with no attempt made to remove dynastically related mutations from the calculation.

Table 1 **Vλ mutations in Ugi-expressing and control DT40 transfectants**

| Clone | Expansion (weeks) | Sequences | | Total mutations | Mutations at dC/dG | | |
|---|---|---|---|---|---|---|---|
| | | Number | Mutations per sequence | | Ts | Tv | % Ts |
| DT-Ugi1 | 3 | 17 | 1.4 | 24 | 21 | 2 | 91 |
| DT-Ugi2 | 3 | 22 | 1.1 | 24 | 19 | 5 | 79 |
| DT-Ugi3 | 5 | 53 | 1.1 | 56 | 44 | 11 | 80 |
| DT-Ugi4 | 5 | 58 | 0.7 | 38 | 31 | 7 | 82 |
| DT-Ugi5 | 7 | 8 | 2.1 | 17 | 15 | 2 | 88 |
| DT-Ugi6 | 7 | 30 | 0.6 | 17 | 14 | 3 | 82 |
| DT-Ugi7 | 3 | 62 | 0.5 | 28 | 25 | 2 | 93 |
| DT-Ugi7 | 8 | 21 | 1.3 | 28 | 23 | 2 | 92 |
| Pooled DT-Ugi clones | | 271 | 1.1 ± 0.6 | 221 | 183 | 33 | 86 ± 6 |
| DT-Con1 | 3 | 49 | 0.5 | 23 | 10 | 10 | 50 |
| DT-Con2 | 3 | 30 | 0.8 | 24 | 4 | 20 | 17 |
| DT-Con3 | 5 | 33 | 0.8 | 28 | 12 | 13 | 48 |
| DT-Con4 | 5 | 45 | 0.6 | 27 | 10 | 15 | 40 |
| DT-Con5 | 5 | 94 | 0.4 | 39 | 16 | 20 | 44 |
| DT-Con6 | 5 | 43 | 0.6 | 26 | 12 | 12 | 50 |
| DT-Con7 | 3 | 57 | 0.4 | 22 | 6 | 16 | 27 |
| DT-Con7 | 8 | 21 | 1.2 | 26 | 7 | 18 | 28 |
| Pooled DT-Con clones | | 372 | 0.6 ± 0.2 | 210 | 77 | 119 | 38 ± 13 |

Ts, transitions; Tv, transversions. In compiling the total number of mutations in each individual transfectant population, the same criterion used in Fig. 2b was applied to avoid counting the same mutational event twice. In calculating the total mutations in the pool of DT-Ugi and DT-Con clones, mutations common to the DT-Ugi7 (and DT-Con7) transfectants as analysed at 3 and 8 weeks have been counted only once. The average ± s.d. of mutations per sequence and % Ts are indicated for the pooled clones.

the nucleotide substitutions at dC/dG were transitions in the control transfectants (with the percentage in individual clones ranging from 17% to 50%), the percentage of transitions increased to a mean value of 86% in *Ugi* transfectants (79–93% in individual clones). It also seems that the Ugi-expressing clones accumulate slightly more mutations than control transfectants (despite the generation times of the Ugi-expressing transfectants averaging 2–3 h longer than controls; data not shown). Ugi expression, however, has had little effect on the distribution of mutations along the V gene segment, with 38% of the mutations occurring within an RGYW/WRCY nucleotide consensus (where R is purine, Y is pyrimidine and W is A or T) compared with 33% in controls[6] (these percentages increase to 53% and 50%, respectively, if the consensus is restricted to RGY/RCY).

The effects of Ugi on the nature of the mutations accumulated within the IgV gene are likely to be through perversion of the pathway of antibody hypermutation in these cells, rather than a general mutagenic effect of inhibiting uracil-DNA glycosylase[17]. The mutations observed in Ugi-expressing cells are specific to the IgV gene segment: no mutations were found in either the Igλ constant region or in a control gene. Thus, no mutations were detected in PCR-amplified genomic clones that covered either Cλ (a stretch of 234 base pairs; 23 clones analysed) or a 540-base-pair portion of the *AID* gene (23 clones analysed). Similarly, introduction of *Ugi* into *AID*-deficient DT40 cells[18] did not cause a mutator phenotype at the IgV locus because, like the parental *AID*-deficient DT40 cells, the *Ugi*-transfected *AID*-deficient cells did not give rise to sIgM-loss variants (the percentage of IgM-loss variants after 3 weeks was below the background detection level of 0.02% in both cases; data not shown).

## Discussion

Inhibition of uracil-DNA glycosylase in *XRCC2*-deficient DT40 cells results in a small increase in the rate of mutation fixation within the Vλ gene as well as a dramatic shift in the pattern of nucleotide substitutions at dC/dG from 38% to 86% transitions. The increased mutation rate could indicate that, in the absence of Ugi, a proportion of the dU residues in the IgV gene that have been generated by dC deamination are repaired: in the presence of Ugi, the repair pathway is now shifted into phase 1A mutation. It is equally possible that the increased mutation rate in the *Ugi* transfectants reflects the fact that whereas replication of the dU/dG pair (phase 1A) will always be mutagenic, replication over the abasic site (phase 1B) need not be mutagenic, depending on the nucleotide inserted opposite the abasic site. At present, we cannot discriminate between these two possibilities.

However, the transition shift effected by inhibition of uracil-DNA glycosylase is readily explained by a shift from predominantly phase 1B mutation to predominantly phase 1A mutation. The reason why only 80–90% (rather than 100%) of the dC/dG mutations in Ugi-expressing cells are transitions is unclear. It could well be that not all uracil excision activity has been inhibited in these cells. Alternatively, even when uracil excision activity is inhibited, the cells might have available to them some other mutagenic pathway for processing or replicating past the dU in dU/dG lesions. In any case, the result gives a strong indication that IgV gene diversification does indeed proceed by a pathway involving the processing of dU residues generated by dC deamination within the Ig locus itself. □

## Methods

### Cell culture, transfection and mutation analysis

DT40 subclone CL18 cells[19,20], its sIgM-positive derivative[6] clone 4 as well as *XRCC2*-deficient[5] and *AID*-deficient[18] mutants were maintained as previously described[6]. Mouse L-M*tk*$^-$ fibroblasts were from our lab collection. The *Ugi* gene from *Bacillus subtilis* bacteriophage PBS2 (a gift from R. Savva) was cloned into the polylinkers of vector pIRESpuro 2 (Clontech) as well as into a derivative[21] of pEAK8 (Edge Biosystems); an additional hygromycin-resistance cassette was then inserted into the *Bam*HI site to yield pIRES-Ugi and pEF-Ugi. The plasmids were linearized (pIRES-Ugi, *Pvu*I; pEF-Ugi, *Mlu*I) and transfected into *XRCC2*-deficient DT40 by electroporation[6,18]; clones were selected in 1.5 mg ml$^{-1}$ hygromycin B (ICN) or 0.25 mg ml$^{-1}$ puromycin (Sigma).

The generation of sIgM-loss variants was analysed by flow cytometry and such variants were purified by cell sorting[6]. The rearranged Vλ was amplified by PCR from genomic DNA using Pfu Turbo polymerase (Stratagene), cloned into M13mp18, and sequenced and analysed for mutation as previously[6].

### Uracil-DNA glycosylase assay

Exponentially growing cells were collected, washed in PBS buffer, resuspended in 25 mM Hepes, 5 mM EDTA, 1 mM dithiothreitol and 10% glycerol at pH 7.8 (HED buffer) with complete protease inhibitors (Roche) at about $10^5$ cells μl$^{-1}$ and lysed by sonication (five 15-s pulses). After centrifugation at 10,000*g* for 20 min at 4 °C, the supernatant was frozen in aliquots into liquid $N_2$ and stored at −80 °C. Uracil-DNA glycosylase assays were carried out in HED buffer by mixing clarified whole-cell extract (10 μg of total protein at the highest concentration) with 1 pmol of fluorescein-labelled oligonucleotide substrate in a final volume of 10 μl for 2 h at 37 °C. This double-stranded oligonucleotide with a single dU/dG mismatch was made by annealing 5′-ATTATTATTATTCCGUGGATTTATTTA TTTATTTATTTATTT-fluorescein to the complementary oligonucleotide, 5′-AAATAA ATAAATAAATAAATAAATCCGCGGAATAATAATAAT. The reaction was terminated by the addition of 10 μl of formamide loading dye (Amersham Pharmacia) and the products were resolved on 15% TBE-urea polyacrylamide gels. The reaction products were visualized using a Typhoon phosphorimager (Amersham Pharmacia). The existing AP endonuclease activity present in the extracts was sufficient to cleave all the deglycosylated substrate generated during the reaction. This was confirmed by performing parallel experiments in which the reaction was treated at the end of the incubation with *Escherichia coli* endonuclease IV (Trevigen) or alkali. In some experiments, the extract was pre-

incubated with purified Ugi (New England Biolabs) as indicated for 10 min on ice before adding the oligonucleotide substrate.

Received 28 June; accepted 16 July 2002; doi:10.1038/nature00981.
Published online 31 July 2002.

1. Petersen-Mahrt, S. K., Harris, R. S. & Neuberger, M. S. AID mutates *E. coli* suggesting a DNA deamination mechanism for antibody diversification. *Nature* **418,** 99–103 (2002).
2. Muramatsu, M. *et al.* Specific expression of activation-induced cytidine deaminase (AID), a novel member of the RNA-editing deaminase family in germinal center B cells. *J. Biol. Chem.* **274,** 18470–18476 (1999).
3. Lindahl, T. Suppression of spontaneous mutagenesis in human cells by DNA base excision-repair. *Mutat. Res.* **462,** 129–135 (2000).
4. Lindahl, T. An N-glycosidase from *Escherichia coli* that releases free uracil from DNA containing deaminated cytosine residues. *Proc. Natl Acad. Sci. USA* **71,** 3649–3653 (1974).
5. Takata, M. *et al.* Chromosome instability and defective recombinational repair in knockout mutants of the five Rad51 paralogs. *Mol. Cell. Biol.* **21,** 2858–2866 (2001).
6. Sale, J. E., Calandrini, D. M., Takata, M., Takeda, S. & Neuberger, M. S. Ablation of XRCC2/3 transforms immunoglobulin V gene conversion into somatic hypermutation. *Nature* **412,** 921–926 (2001).
7. Lindahl, T. Instability and decay of the primary structure of DNA. *Nature* **362,** 709–715 (1993).
8. Pearl, L. H. Structure and function in the uracil-DNA glycosylase superfamily. *Mutat. Res.* **460,** 165–181 (2000).
9. Nilsen, H. *et al.* Uracil-DNA glycosylase (UNG)-deficient mice reveal a primary role of the enzyme during DNA replication. *Mol. Cell* **5,** 1059–1065 (2000).
10. Haushalter, K. A., Todd Stukenberg, M. W., Kirschner, M. W. & Verdine, G. L. Identification of a new uracil-DNA glycosylase family by expression cloning using synthetic inhibitors. *Curr. Biol.* **9,** 174–185 (1999).
11. Nilsen, H. *et al.* Excision of deaminated cytosine from the vertebrate genome: role of the SMUG1 uracil-DNA glycosylase. *EMBO J.* **20,** 4278–4286 (2001).
12. Friedberg, E. C., Ganesan, A. K. & Minton, K. N-glycosidase activity in extracts of *Bacillus subtilis* and its inhibition after infection with bacteriophage PBS2. *J. Virol.* **16,** 315–321 (1975).
13. Wang, Z. & Mosbaugh, D. W. Uracil-DNA glycosylase inhibitor of bacteriophage PBS2: cloning and effects of expression of the inhibitor gene in *Escherichia coli*. *J. Bacteriol.* **170,** 1082–1091 (1988).
14. Karran, P., Cone, R. & Friedberg, E. C. Specificity of the bacteriophage PBS2 induced inhibitor of uracil-DNA glycosylase. *Biochemistry* **20,** 6092–6096 (1981).
15. Mol, C. D. *et al.* Crystal structure of human uracil-DNA glycosylase in complex with a protein inhibitor: protein mimicry of DNA. *Cell* **82,** 701–708 (1995).
16. Handa, P., Roy, S. & Varshney, U. The role of leucine 191 of *Escherichia coli* uracil DNA glycosylase in the formation of a highly stable complex with the substrate mimic, Ugi, and in uracil excision from the synthetic substrates. *J. Biol. Chem.* **276,** 17324–17331 (2001).
17. Radany, E. H. *et al.* Increased spontaneous mutation frequency in human cells expressing the phage PBS2-encoded inhibitor of uracil-DNA glycosylase. *Mutat. Res.* **461,** 41–58 (2000).
18. Harris, R. S., Sale, J. E., Petersen-Mahrt, S. K. & Neuberger, M. S. AID is essential for immunoglobulin V gene conversion in a cultured B cell line. *Curr. Biol.* **12,** 435–438 (2002).
19. Baba, T. W., Giroir, B. P. & Humphries, E. H. Cell lines derived from avian lymphomas exhibit two distinct phenotypes. *Virology* **144,** 139–151 (1985).
20. Buerstedde, J. M. *et al.* Light chain gene conversion continues at high rate in an ALV-induced cell line. *EMBO J.* **9,** 921–927 (1990).
21. Harris, R. S., Croom-Carter, D. S., Rickinson, A. B. & Neuberger, M. S. Epstein–Barr virus and the somatic hypermutation of immunoglobulin genes in Burkitt's lymphoma cells. *J. Virol.* **75,** 10488–10492 (2001).

**Supplementary Information** accompanies the paper on *Nature*'s website (http://www.nature.com/nature).

## Acknowledgements

We thank R. Savva for the *Ugi* cassette, S. Takeda for *XRCC2*-deficient DT40 cells, R. Grenfell for help with cell sorting, and R. Harris, S. Petersen-Mahrt, C. Rada and J. Sale for discussions. J.D.N. was supported by a César Milstein fellowship and the Fundación Antorchas, Argentina.

## Competing interests statement

The authors declare that they have no competing financial interests.

Correspondence and requests for materials should be addressed to M.S.N. (e-mail: msn@mrc-lmb.cam.ac.uk).